Radiology

REVIEWS AND COMMENTARY • REVIEW

Imaging Diagnosis and Follow-up of Advanced Prostate Cancer: Clinical Perspectives and State of the Art

Raquel Perez-Lopez, MD, PhD • Nina Tunariu, MD, FRCR* • Anwar R. Padhani, MBBS, FRCR • Wim J. G. Oyen, MD, PhD • Stefano Fanti, MD • Hebert Alberto Vargas, MD • Aurelius Omlin, MD • Michael J. Morris, MD • Johann de Bono, MBCHB, PhD • Dow-Mu Koh, MD, FRCR*

From the Radiomics Group, Vall D'Hebron Institute of Oncology, Barcelona, Spain (R.P.L.); Departments of Radiology (N.T., D.M.K.) and Nuclear Medicine (W.J.G.O.), Royal Marsden NHS Foundation Trust, Downs Road, Sutton SM2 5PT, England; Paul Strickland Scanner Centre, Mount Vernon Hospital, Northwood, England (A.R.P.); Divisions of Radiotherapy and Imaging (W.J.G.O., D.M.K.) and Clinical Studies & Prostate Cancer Targeted Therapy Group (J.d.B.), Institute of Cancer Research, Sutton, England; Departments of Radiology (S.F.) and Genitourinary Oncology Service and Medicine (M.J.M.), Memorial Sloan-Kettering Cancer Center, New York, NY; Department of Oncology and Haematology, Cantonal Hospital St. Gallen, St. Gallen, Switzerland (H.A.V., A.O.); Department of Medical Oncology, Inselspital, Bern University Hospital, University of Bern, Switzerland (H.A.V., A.O.); and Department of Medicine, Weill Cornell Medicine, New York, NY (M.J.M.). Received September 11, 2018; revision requested October 22; revision received February 4, 2019; accepted February 11. **Address correspondence to** D.M.K. (e-mail: *dowmukoh@icr.ac.uk*).

Supported by the National Institute for Health Research Biomedical Research Centre & Clinical Research Facility.

*R.P.L. and N.T. contributed equally to this work.

Conflicts of interest are listed at the end of this article.

Radiology 2019; 292:273–286 • https://doi.org/10.1148/radiol.2019181931 • Content code: GU

The management of advanced prostate cancer has changed substantially with the availability of multiple effective novel treatments, which has led to improved disease survival. In the era of personalized cancer treatments, more precise imaging may help physicians deliver better care. More accurate local staging and earlier detection of metastatic disease, accurate identification of oligometastatic disease, and optimal assessment of treatment response are areas where modern imaging is rapidly evolving and expanding. Next-generation imaging modalities, including whole-body MRI and molecular imaging with combined PET and CT and combined PET and MRI using novel radiopharmaceuticals, create new opportunities for imaging to support and refine management pathways in patients with advanced prostate cancer. This article demonstrates the potential and challenges of applying next-generation imaging to deliver the clinical promise of treatment breakthroughs.

© RSNA, 2019

Online supplemental material is available for this article.

Online SA-CME • *See www.rsna.org/learning-center-ry*

Learning Objectives:

After reading the article and taking the test, the reader will be able to:

- List the role of imaging in advanced prostate cancer evaluation and the limitations of the standard imaging for diagnosis, staging, and response assessment
- Identify the emerging role of advanced imaging in evaluating oligometastatic disease, including the growing importance of imaging in the evaluation of bone response to treatment
- Identify the emerging roles of novel radiopharmaceuticals and theranostics in patient care

Accreditation and Designation Statement

The RSNA is accredited by the Accreditation Council for Continuing Medical Education (ACCME) to provide continuing medical education for physicians. The RSNA designates this journal-based SA-CME activity for a maximum of 1.0 *AMA PRA Category 1 Credit™*. Physicians should claim only the credit commensurate with the extent of their participation in the activity.

Disclosure Statement

The ACCME requires that the RSNA, as an accredited provider of CME, obtain signed disclosure statements from the authors, editors, and reviewers for this activity. For this journal-based CME activity, author disclosures are listed at the end of this article.

Advanced prostate cancer comprises several clinicopathologic states characterized as incurable due to the presence of locally advanced or metastatic disease. The disease is considered locally advanced when it has extended beyond the confines of the prostate gland, which can also involve adjacent structures or pelvic lymph nodes. Metastatic prostate cancer occurs when the disease has spread to sites remote from the primary tumor (eg, bones or distant lymph nodes); it is a fatal condition, with a 5-year relative survival rate of about 30% (1). Because treatment-naive prostate cancers are sensitive to hormonal treatment (also known as hormone-sensitive prostate cancer), combination treatments with androgen deprivation therapy are the mainstay treatments for advanced and metastatic prostate cancer at initial diagnosis. Patients who have disease progression while undergoing androgen deprivation therapy enter a clinical state called castration-resistant prostate carcinoma (CRPC). The prevalence of metastatic disease is greatest in men with high risk (according to established clinical and pathologic criteria) and locally advanced disease and in those with castration-resistant disease. Patients who have CRPC with rising prostate-specific antigen (PSA) levels and without metastases that can be detected with imaging (CT or bone scans) are classified as having M0 CRPC disease and are considered to have advanced prostate cancer (Fig E1 [online]).

This copy is for personal use only. To order printed copies, contact *reprints@rsna.org*

Abbreviations

CRPC = castration-resistant prostate cancer, DW = diffusion weighted, FDG = fluorodeoxyglucose, FDHT = 16-β-fluoro-5-α-dihydrotestosterone, MET-RADS-P = METastasis Reporting and Data System for Prostate Cancer, PSA = prostate-specific antigen, PSMA = prostate-specific membrane antigen, RECIST = Response Evaluation Criteria In Solid Tumors, SUV = standardized uptake value, USPIO = ultrasmall superparamagnetic iron oxide

Summary

Whole-body diffusion-weighted MRI and molecular imaging will play increasing roles in defining the presence and extent of metastatic disease, enabling assessment of treatment response and disease progression, and will improve our understanding of disease biology.

Essentials

- Conventional imaging with CT and bone scanning has limited sensitivity to depict nodal and bone disease in prostate cancer.
- Next-generation imaging, including whole-body diffusion-weighted MRI with novel radiopharmaceuticals for combined PET and CT and combined PET and MRI, is more accurate in defining the presence and extent of disease.
- Next-generation imaging enables earlier initiation of treatment in patients with occult metastatic disease at CT and bone scanning; optimal change in treatment via earlier detection of disease progression; detection of oligometastatic state (limited metastatic disease), which may be treated more aggressively; guidance of tissue biopsies for molecular tumor characterization; and development of novel predictive and prognostic biomarkers to guide therapies.

Research has shown considerable inter- and intrapatient heterogeneity of disease biology at the genetic and molecular levels (2), with advancing disease before and during therapy. Tumor heterogeneity is thought to underlie response heterogeneity to treatments, contributing to the development of resistance. The increasing number of life-prolonging therapies for advanced prostate cancer demands improved molecular stratification and predictive biomarkers to optimize patient treatment. Emerging predictive molecular biomarkers to new therapies include *BRCA* gene mutation, androgen receptor splice variants (3), phosphatase and tensin homolog loss (4), homologous recombination deoxyribonucleic acid repair defects (5), and mismatch repair defects (6). Modern imaging contributes to advanced prostate cancer management by defining the presence and extent of tumor, enabling imaging-targeted metastatic disease sampling, depicting disease response, and allowing earlier detection of treatment failure. Modern imaging, together with imaging-targeted tissue sampling and molecular biomarkers, can improve the understanding of prostate cancer biology by elucidating the development of therapy resistance and evolution of metastases (6,7).

In this review, we discuss the roles of established (CT and bone scanning) and next-generation imaging technologies, including whole-body MRI and PET, combined PET and CT, and combined PET and MRI, in defining the presence and extent of disease to support modern advanced prostate cancer management. We discuss the emerging role of imaging in the evaluation of oligometastatic disease, recognize the growing importance of imaging in the evaluation of disease response to treatment, and appreciate the potential for imaging theranostics in guiding patient care. Some of the potential and challenges of next-generation imaging are also discussed.

Advanced Prostate Cancer Imaging at Staging and during Follow-up

Imaging investigations of prostate cancer are more informative when physicians have knowledge of a patient's clinical findings and symptoms, risk status, likely testosterone level, and perceived risk of metastatic disease. When we apply the National Comprehensive Cancer Network, or NCCN, 2018 (8) and European Association of Urology, European Society for Radiotherapy and Oncology, and International Society of Geriatric Oncology (hereafter, EAU-ESTRO-SIOG) (9) management guidelines, patients who present with intermediate- or high-risk locally advanced disease are usually referred for imaging to detect metastatic disease (Fig 1). Imaging is also performed when disease relapse is suspected, usually based on rising serum PSA levels (biochemical recurrence), in patients who have undergone curative treatment (8,9). Once disease is confirmed, subsequent imaging is performed to assess therapy response and complications. The frequency of imaging assessment is guided by the prostate cancer state (hormone sensitive or castration resistant), anatomic location, and extent of metastatic disease (Fig 2).

The volume of disease at presentation and during initial biochemical recurrence and biochemical failure while undergoing systemic therapy are highly prognostic, affecting therapy options. In patients with only a few (≤5) demonstrable sites of metastatic disease described as oligometastatic disease (10), more aggressive metastasis-directed treatments can be considered, such as targeted radiation therapy, surgery, or local ablative procedures. However, the impact of such treatments is still being investigated (11).

Systemic treatment responses are usually monitored with a combination of imaging, clinical assessments, measurement of the serum PSA level, and evaluation of other biochemical indexes. Imaging plays a relatively minor role if patients are responding clinically and with blood biomarkers in those with hormone-sensitive states. If first-line androgen deprivation therapy becomes ineffective, patients move into a CRPC state (with suppressed serum testosterone levels). This situation is associated with a high incidence of metastatic disease; thus, other life-prolonging or palliative therapies are considered. Patients with CRPC who do not have metastatic disease that is visible at imaging can also be considered for newer therapies (12).

Imaging Assessment of Advanced Prostate Cancer

Prostate cancer has a propensity to spread to the bones, lymph nodes, liver, lungs, and—rarely—brain (13,14). Up to 62% of patients with newly diagnosed metastatic prostate cancer (13) and more than 40% of patients with CRPC (14) have metastatic disease confined to the skeletal system. When patients undergo multiple treatments with different drugs, vis-

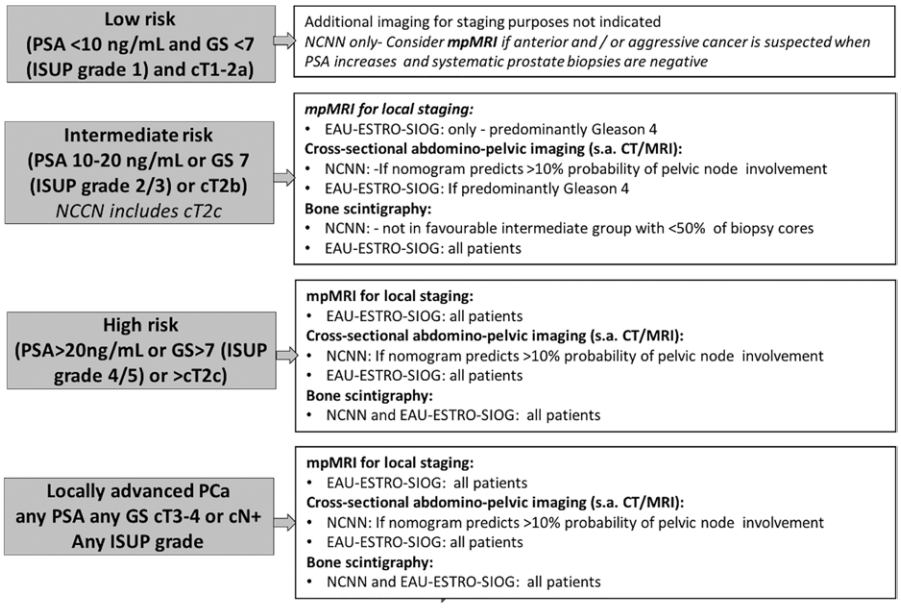

Figure 1: Schematic shows patient and imaging pathways for disease staging. Recommendations are based on National Comprehensive Cancer Network (NCCN) guidelines, version 3.2018, and European Association of Urology, European Society for Radiotherapy and Oncology, and International Society of Geriatric Oncology (EAU-ESTRO-SIOG) guidelines 2017.

ceral metastases and unusual sites of metastatic involvement become more frequent. Both CT and bone scanning have limited ability to depict the heterogeneity of response behavior of metastatic and local disease, thereby contributing to therapy failure and poor patient outcome (15). Hence, there is growing interest in next-generation imaging techniques, such as whole-body MRI and PET/CT and PET/MRI using a variety of radiopharmaceuticals (Table), to improve disease assessment. The proposed roles of imaging in the management of advanced prostate cancer are summarized in Table E1 (online). The table shows that in patients with advancing disease, there are multiple key clinical issues that can be affected by imaging. These include identifying the presence and extent of metastases, assessing treatment response, and potentially providing predictive and prognostic biomarkers for therapy selections and allowing identification of metastases that can be biopsied for genomic or molecular categorization.

Detection of Metastatic Nodal Disease

Conventional CT imaging.—The performance of conventional CT in the detection of lymph node involvement based on size criteria is poor (16) since there is significant overlap in the size of benign reactive and metastatic lymph nodes. On the basis of size, the diagnostic sensitivity of CT (and conventional anatomic T1- or T2-weighted MRI) sequences in the detection of nodal metastases (0.5–2 cm in shorter axis) is less than 40% in patients with prostate cancer (16,17) because of the high prevalence of micrometastases. For this reason, the decision to perform nodal dissection during primary prostate cancer surgery has been largely guided by clinical nomography. Imaging has been used to guide nodal dissections to suspicious sites outside the "normal surgical field" (9,18,19). Molecular and functional imaging techniques are being investigated to improve the accuracy of nodal metastasis detection and to guide nodal sampling at surgery (20).

MRI.—Diffusion-weighted (DW) MRI is sensitive to differences in the mobility of water between tissues and enables calculation of the apparent diffusion coefficient (ADC). Malignant nodes return lower ADC values than do benign lymph nodes, but there is overlap of ADC values between malignant and nonmalignant nodes (21). On per-patient level and per–pelvic side-wall nodes level subanalyses, negative likelihood ratios are not low enough to avoid or lateralize lymphadenectomy. This is relevant as pelvic side-wall nodes are the most frequent site of metastatic disease from prostate cancer and define the extension of surgery. However, positive likelihood ratios are sufficiently high to increase the extent of planned lymphadenectomy or prophylactic pelvic nodal irradiation if suspicious nodes are seen outside planned surgical or radiation therapy fields (21). There has been hope that use of a lymphotrophic ultrasmall superparamagnetic iron oxide (USPIO) MRI contrast medium (Fig 3) (22,23) can improve malignant lymph node detection, especially when combined with DW imaging (22,23). Meta-analysis showed that DW MRI with a USPIO had higher diagnostic sensitivity compared with conventional MRI without the USPIO (24). In a study evaluating 2993 normal-size lymph nodes in patients with prostate or bladder cancer, combining DW MRI with a USPIO improved diagnostic sensitivity and specificity (range, 65%–75% and 93%–96%, respectively) compared with sensitivity and specificity of MRI with a USPIO alone (range, 55%–65% and 71%–91%, respectively) (22). However, USPIO MRI did not demonstrate clinical utility in phase III studies, and it remains commercially unavailable for nodal imaging.

PET/CT and PET/MRI.—Fluorine 18 (^{18}F) fluorodeoxyglucose (FDG) has poor performance in patients with prostate cancer (25) because prostate cancer cells are usually not glucose avid. In contrast, radiolabeled choline derivatives (eg, carbon 11 [^{11}C] and ^{18}F choline) that are used to detect increased cell membrane turnover are effective prostate cancer PET tracers. In a meta-analysis of 609 patients, the sensitivity and specificity of ^{11}C and ^{18}F choline PET/CT for pelvic lymph node metastases were 62% and 92%, respectively (Fig 4) (26). Another

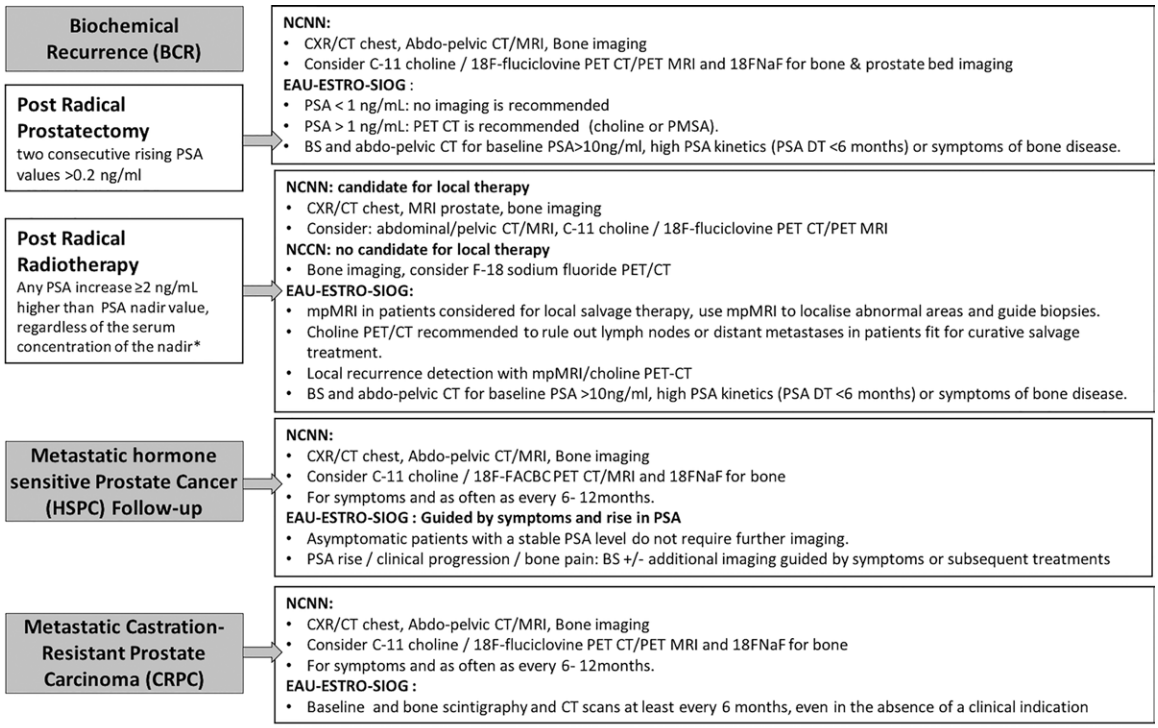

Figure 2: Schematic shows patient and imaging pathways for follow-up. Recommendations are based on National Comprehensive Cancer Network (NCCN) guidelines, version 3.2018, and European Association of Urology, European Society for Radiotherapy and Oncology, and International Society of Geriatric Oncology (EAU-ESTRO-SIOG) guidelines 2017.

Summary of the Targets, Strengths, and Weaknesses of PET/CT and PET/MRI Radiopharmaceuticals Widely Used to Assess Advanced Prostate Cancer

Radiopharmaceutical	Target	Strength	Weakness
^{18}F FDG	Glucose metabolism	Tracer activity may identify highly aggressive tumors	Poor performance in prostate cancer, prostate cancer cells are usually not glucose avid
^{11}C and ^{18}F choline	Cell membrane turnover	Can be used to visualize both soft-tissue and bone disease	Limited sensitivity for liver metastases detection because of high tracer uptake in the normal liver
^{68}Ga PSMA	Cell membrane protein expressed in prostate cancer	High sensitivity in the detection of nodal disease, promising detection rates in prostate cancer with low PSA or PSA doubling time	Limited evidence from literature on real impact on patient survival, PSMA expression is increased with antiandrogen therapy
^{18}F NaF	Bone turnover	High sensitivity for bone metastases detection	Bone disease specific, cannot be used to assess soft-tissue disease
^{18}F FDHT	Binds to the androgen receptor	Indicator of wild-type androgen receptor expression, may be useful as a response indicator to androgen deprivation therapy	Lack of ligand binding due to generation of androgen receptor splice variants when prostate cancer develops resistance to androgen deprivation therapy

Note.—FDG = flurodeoxyglucose, FDHT = fluorodihyrotestosterone, PSMA = prostate-specific membrane antigen, NaF = sodium fluoride.

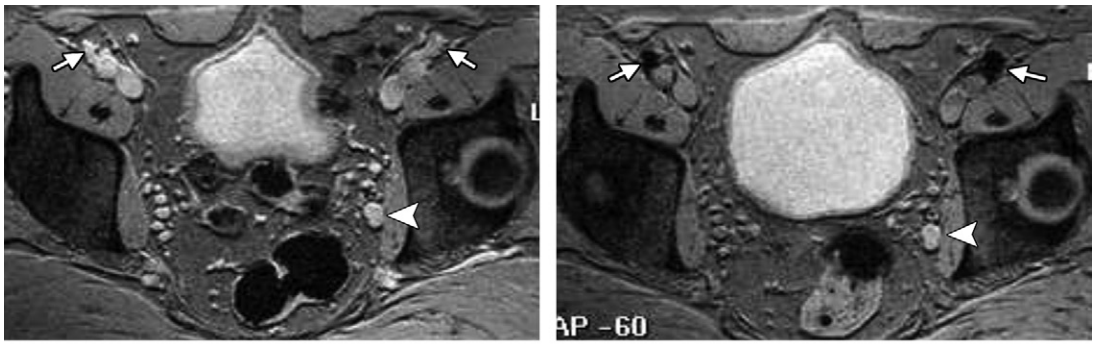

a. b.

Figure 3: Ultrasmall superparamagnetic iron oxide (USPIO) MRI was used to detect nodal disease in a 65-year-old man with prostate cancer. **(a, b)** Axial T2*-weighted MRI (multi-echo data image combination, or MEDIC) before (**a**) and after (**b**) USPIO administration (intravenous feuromoxtran, 0.13 mL per kilogram of body weight) shows normal nodal contrast material uptake in normal external iliac lymph nodes (arrows), with reduced nodal signal after contrast material administration. On the other hand, a malignant left obturator node (arrowhead) shows no appreciable signal reduction after USPIO contrast material administration (Images courtesy of Dr Aslam Sohaib.)

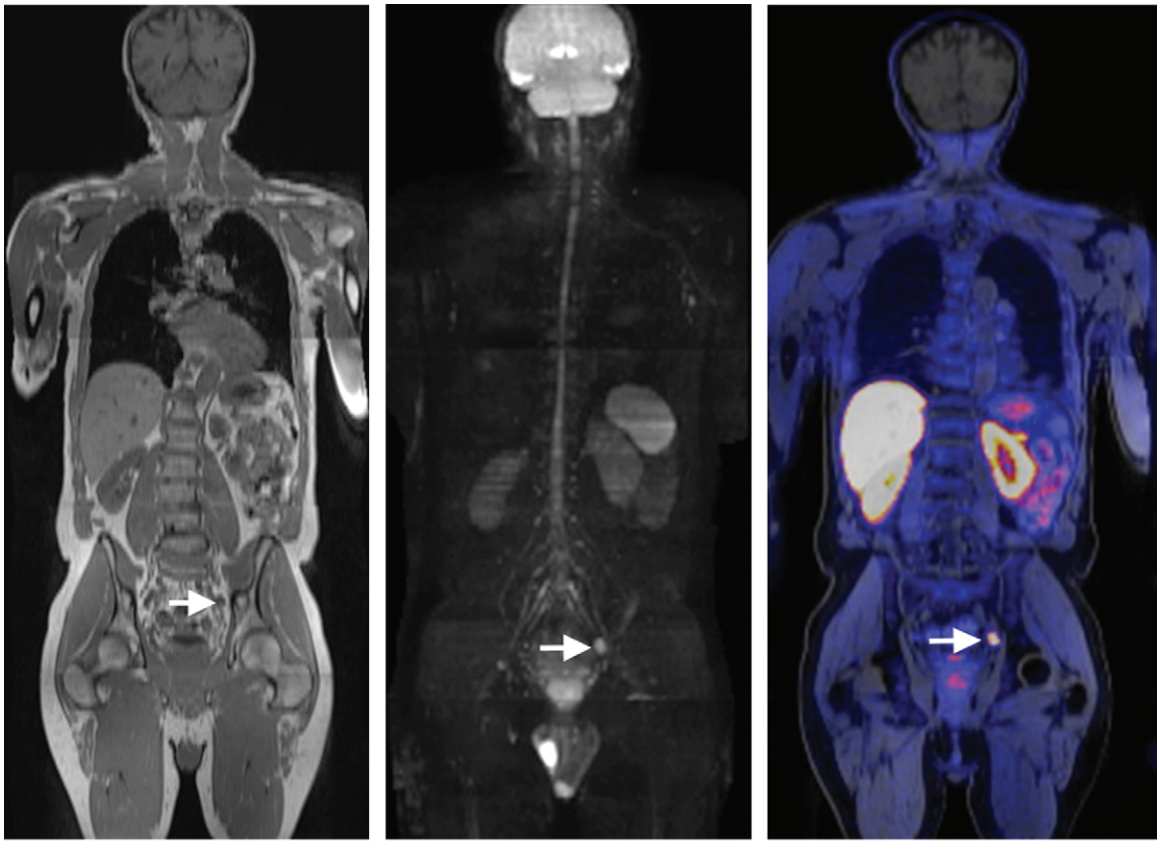

a. b. c.

Figure 4: A 63-year-old man with high-risk Gleason 4+3 prostate cancer underwent fluorine 18 (^{18}F) choline PET/MRI to detect malignant nodal disease. **(a)** Coronal T1-weighted PET/MRI shows a 1-cm node (arrow) in the left pelvic sidewall. **(b)** Coronal diffusion-weighted MRI (*b* value = 900 sec/mm^2) shows impeded diffusion (arrow). **(c)** Coronal fusion ^{18}F choline and T1-weighted MRI shows increased tracer activity within the node (arrow), suggesting disease involvement. (Images courtesy of Dr Gary Cook.)

meta-analysis by Evangelista et al (27) in 441 patients undergoing nodal staging with ^{11}C and ^{18}F choline PET reported a pooled sensitivity of 49.2% and a specificity of 95%. More recently, gallium 68 (^{68}Ga) prostate surface membrane antigen (PSMA) PET/CT has shown higher sensitivity in the detection of nodal disease. PSMA is a cell surface enzyme, which is overexpressed in patients with prostate cancer. While the name suggests that the protein is prostate specific, the protein is also expressed by the lacrimal gland, salivary gland, proximal renal tubules, small intestine, and neovasculature of the thyroid and renal neoplasms (28). In patients with prostate cancer, greater PSMA expression is seen with higher Gleason score (29) in

castration-resistant tumors and with androgen deprivation therapy (30). In a meta-analysis of five retrospective studies with pathology-proven disease, ^{68}Ga PMSA had combined sensitivities and specificities of 86% (95% confidence interval: 37%, 98%) and 86% (95% confidence interval: 3%, 100%), respectively, at a patient level (31). In a study of 130 patients at high risk for prostate cancer with histopathologic correlation (32), ^{68}Ga PSMA PET had a sensitivity of 65.9%. The mean size of malignant nodes missed with ^{68}Ga PSMA PET was 3 mm ± 1 (standard deviation). More recently, second-generation ^{18}F-labeled PSMA-directed radiopharmaceuticals with longer half-life, slightly different biodistribution and kinetics, and higher spatial resolution than ^{68}Ga have shown promise for disease staging and biochemical relapse (33). The ^{18}F PSMA can depict metastases in nodes smaller than 8 mm in diameter (34), but additional studies are needed to establish the clinical utility of ^{18}F PSMA tracers.

Detection of Bone Metastases

Standard bone scan and CT.—Technetium 99m (^{99m}Tc) diphosphonate bone scanning is the most widely used method to evaluate bone metastasis presence in patients with prostate cancer. Bone matrix interactions are depicted (osteoblastic activity and increased bone turnover in the vicinity of the metastases). However, early metastases confined to the bone marrow may not show tracer uptake, thereby limiting disease detection. The addition of SPECT to planar imaging, especially when using hybrid SPECT/CT cameras, can improve diagnostic accuracy by reducing the number of equivocal lesions and allows more direct comparison with CT and MRI. A meta-analysis of 1102 patients with prostate cancer comprising 12 studies using $^{99\,m}$Tc planar bone scanning and three studies using SPECT showed a combined sensitivity and specificity for bone metastasis detection of 79% and 82%, respectively, on a per-patient basis. On a per-lesion basis, diagnostic sensitivity and specificity were 59% and 75%, respectively, for planar bone scanning compared with 90% and 85%, respectively, with the addition of SPECT (35).

CT has modest diagnostic accuracy in the detection of bone metastases. This is because small lesions within the bone marrow are difficult to distinguish from the fatty marrow, and substantial bone destruction or new bone formation must occur before lesions can be detected. The pooled sensitivity and specificity of CT in the detection of bone metastases from prostate tumors and other tumor types are reportedly 73% and 95%, respectively (36). However, like many studies reporting on the accuracy of bone scanning, these were conducted without pathologic analysis as the reference standard and in patients with advanced disease, which can bias results toward better diagnostic performance.

In recognition of the fact that both bone scanning (37) and CT (36) result in underestimation of the presence and extent of bone disease, there are implications for patient care, as treatment is increasingly stratified according to disease presence and extent, particularly in patients with oligometastatic disease who frequently receive focal treatments (10). Additionally, recent data have shown that pelvic radiation therapy, traditionally used in patients without metastases, is also effective in patients who present with de novo low-volume disease (38).

For these reasons, whole-body MRI, PET/CT, and PET/MRI are increasingly used to detect bone metastases, with frequent upstaging of the oligometastatic state.

MRI.—When compared with bone scanning and CT, MRI is more accurate in the detection of bone metastases (35) (Fig 5). Whole-body MRI is more sensitive than bone scanning and choline PET/CT in the detection of bone metastases on a per-patient basis, although choline PET/CT showed higher specificity in one study (35). Modern whole-body MRI comprises morphologic sequences (eg, T1- or T2-weighted sequences, short inversion time inversion-recovery sequence), and the addition of DW MRI further improves bone metastasis detection (39–41). Whole-body MRI, including DW MRI, has been shown to be more sensitive and specific than bone scanning in the detection of bone metastases in clinical practice (42), although one recent study showed higher diagnostic performance with ^{68}Ga PSMA (43). Advantages of using a whole-body MRI protocol that comprises both conventional and DW imaging sequences include high detection sensitivity and a more consistent response assessment of bone and visceral metastases through use of the standardized METastasis Reporting and Data System for Prostate Cancer (MET-RADS-P) (44,45). MET-RADS-P recommends standardization of image acquisition and data collection and facilitates detailed recording of the presence, location, and extent of disease. In addition, these techniques are widely available and can be implemented on standard MRI systems. Whole-body MRI, including multiparametric MRI of the prostate, may enable one-modality imaging in patients suspected of having prostate cancer relapse (46) and for primary staging in patients with high risk (40).

PET/CT and PET/MRI.—PET/CT with ^{18}F sodium fluoride (NaF) PET, a bone turnover–specific agent, has higher sensitivity in bone metastases detection compared with planar or SPECT bone scanning (47). However, unlike choline PET/CT, NaF does not accumulate in individuals with nonskeletal disease, and it is less cost-effective than bone scanning; however, it does share the limitations of reduced specificity in the differentiation of malignant from benign osteoblastic uptake.

It is unclear whether choline PET/CT is more sensitive than conventional bone scanning, but it does have higher specificity, with fewer indeterminate bone lesions (26). Wondergem et al (48) found choline PET/CT had better specificity than NaF PET/CT in the detection of bone metastases. At lesion-based analysis, sensitivity and specificity were 84.0% and 97.7%, respectively, with similar results at patient-based analysis (85.2% and 96.5%, respectively). There is limited evidence regarding the performance of ^{68}Ga PSMA PET/CT in the detection of prostate cancer bone metastasis at initial diagnosis. The largest study comparing ^{68}Ga PSMA PET/CT or PET/MRI with bone scanning in 37 patients showed 100% sensitivity for ^{68}Ga PSMA PET/CT and 57% sensitivity for

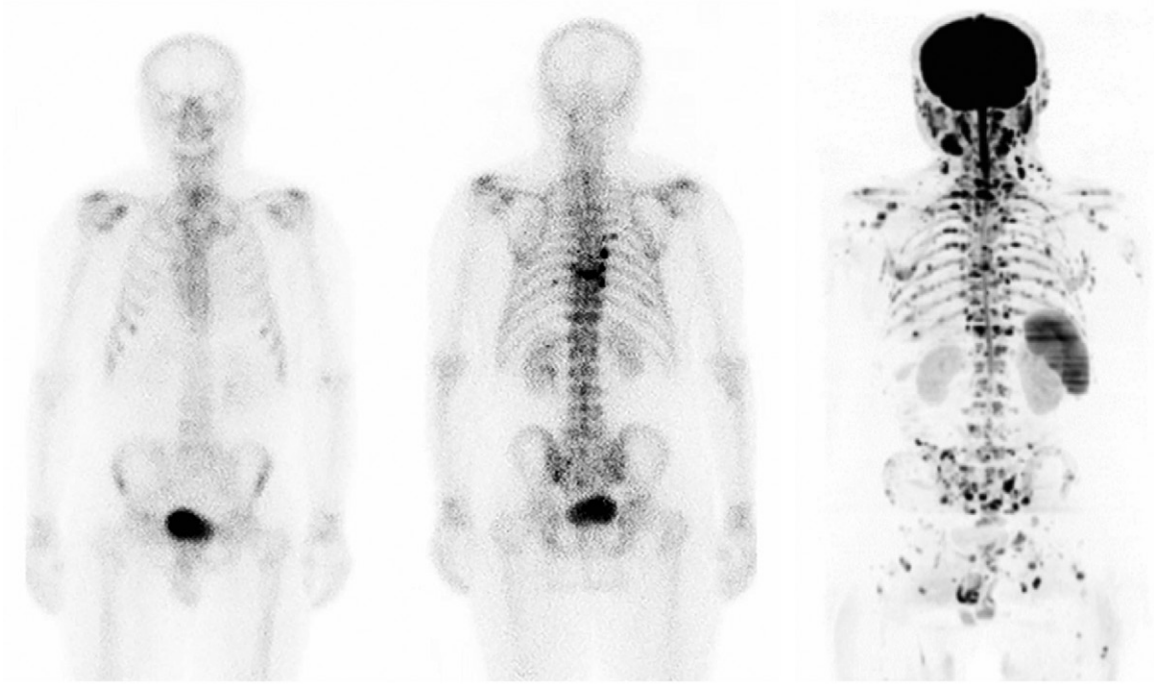

a. b.

Figure 5: Whole-body MRI has higher sensitivity for bone metastases detection in a 71-year-old man with castration-resistant prostate cancer who was receiving antiandrogen targeted therapy and had a rising prostate-specific antigen (PSA) level (109 ng/mL) and a PSA doubling time of 1.5 months. **(a)** Coronal anterior (left) and posterior (right) images obtained with technetium 99m bone scintigraphy. **(b)** Inverted coronal maximum intensity projection whole-body diffusion-weighted (DW) MRI (*b* value = 900 sec/mm^2) shows marked discrepancy between the number of metastatic bone lesions detected, with whole-body DW MRI showing more bone disease as multiple low-signal-intensity focal lesions.

bone scanning; specificity was comparable (100% vs 96%, respectively) (49) (Fig 6), bearing in mind the caveat of absent lesion-based histologic verification.

Other Radiopharmaceuticals to Detect Disease in Advanced Prostate Cancer

The radioconjugate containing a derivative of testosterone, 16-β-fluoro-5-α-dihydrotestosterone (FDHT), and labeled with ^{18}F (^{18}F FDHT) binds to the androgen receptor. In patients with CRPC, ^{18}F FDHT PET/CT has reasonable sensitivity (86%) in disease detection (50) and as an indicator of wild-type androgen receptor expression. It may also indicate response to antiandrogenic drugs (51). However, advancing prostate cancers acquire antiandrogen treatment resistance, with the emergence of androgen-receptor splice variants lacking the ligand binding domain, which can limit the usefulness of this agent.

As prostate cancers upregulate certain amino acid transporters, anti-1-amino-3-^{18}F-fluorocyclobutane-1-carboxylic acid, or FACBC, also known as ^{18}F fluciclovine, is an amino acid analog directed at fatty acid synthesis that has been evaluated as an imaging tracer. A meta-analysis of 251 patients showed pooled sensitivity and specificity of 87% and 66%, respectively (52). Another multicenter study in 596 patients showed sensitivity and specificity of 62.7% and 69.9%, respectively, in the detection of disease relapse (53), which may lead to false-positive results and spurious upstaging of disease because of the lower diagnostic specificity.

The main published meta-analyses and prospective imaging studies of radiopharmaceuticals and MRI in nodal and bone metastases assessment are summarized in Tables E2 and E3 (online).

Oligometastatic Prostate Cancer at Initial Staging and Disease Relapse: Changing Paradigm

The improved performance of prostate cancer–directed next-generation imaging methods (54,55) in the detection of small-volume metastases has enhanced interest in treatment of the oligometastatic state. Oligometastatic disease may be an earlier intermediate stage in cancer spread in between localized disease and widespread metastases. Oligometastatic disease has been defined as no more than five detectable metastases in three clinical scenarios: de novo oligometastatic prostate cancer, oligorecurrent prostate cancer (Fig 7), and oligoprogressive prostate cancer (10,11). Focal treatments, such as radiation therapy or surgery, have been postulated to debulk metastatic tumor and slow disease progression, perhaps delaying the start of systemic treatment (10,11,56). Others, however, have expressed skepticism (57), commenting that the oligometastatic state is merely a feature of limited sensitivity in disease detection (58). Nonetheless, randomized controlled trials are now being conducted to address unanswered questions regarding the treatment of oligometastases and metastases-directed therapies (11) and the role of advanced imaging in this disease setting.

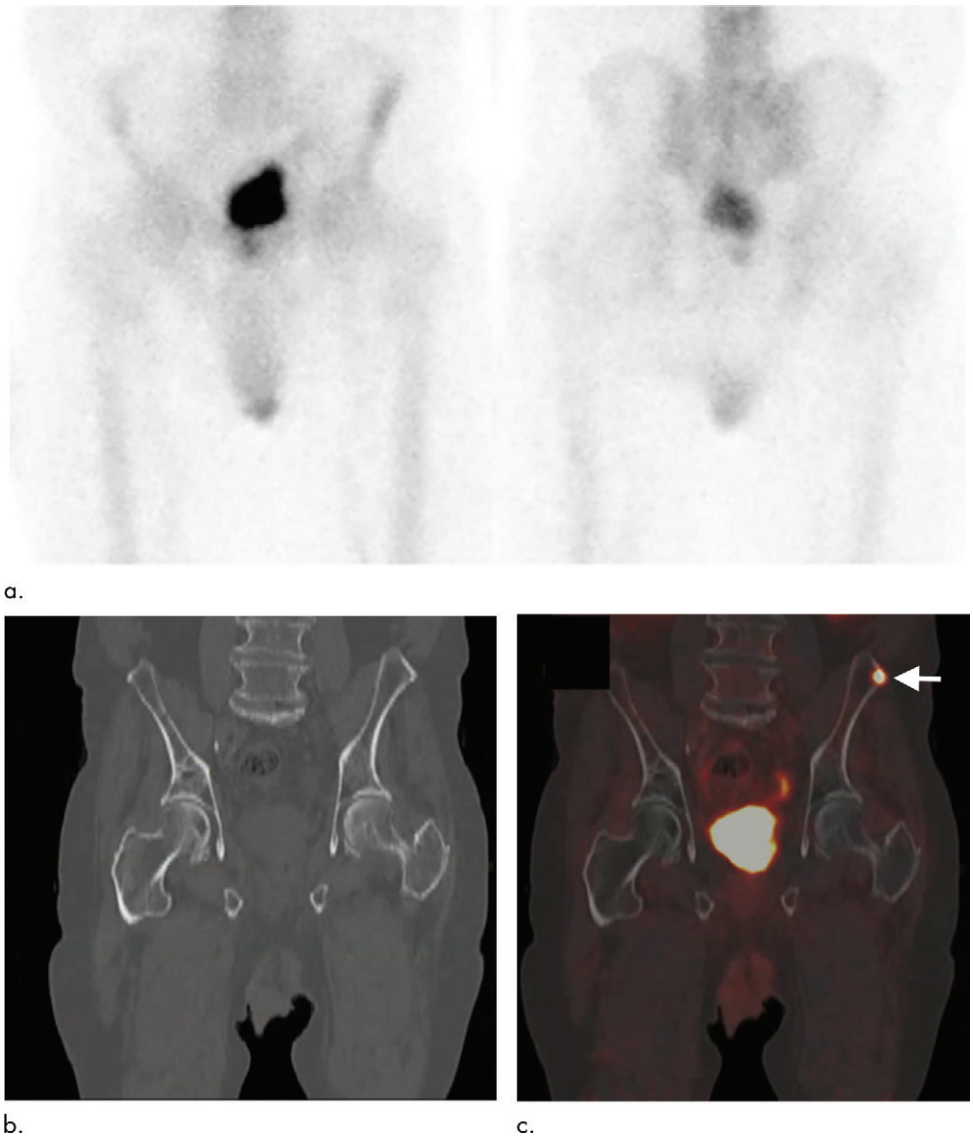

Figure 6: Gallium 68 (^{68}Ga) PET targeting the prostate-specific membrane antigen (PSMA) enables detection of bone metastases not visible at bone scanning in a 100-year-old man with castration-resistant prostate cancer, a rising serum prostate-specific antigen (PSA) level (81 ng/mL), and a PSA doubling time of 2.7 months. **(a)** Coronal anterior (left) and posterior (right) images obtained with technetium 99m scintigraphy. **(b)** Coronal unenhanced CT and **(c)** ^{68}Ga PSMA images show a false-negative result. All images were acquired within 1 month of each other. In **c**, there is a PSMA-avid left anterior iliac crest bone metastasis (arrow) not visible on **a** or **b**, which prompted antiandrogen targeted therapy.

Published data from choline PET/CT (11) and whole-body MRI (55) show that patients with oligometastatis experience relapse most often in the nodes, followed by relapse in bone and viscera. While this finding is encouraging, there is a lack of conclusive evidence on the use of PET/CT or PET/MRI with new prostate cancer–directed radiopharmaceuticals in the management of oligometastatic disease (20,59–61).

Detection of Therapeutic Response

The availability of several effective therapies for advanced prostate cancer has shifted the treatment paradigm toward a more aggressive approach. Overall, measurement of serum PSA level alone to monitor treatment response is not recommended (62), especially in patients with metastatic CRPC because of disease molecular heterogeneity, such that radiologic progression can occur without an increase in PSA level (63) (Fig 8). Thus, imaging is becoming more important in the assessment of treatment benefit in patients with metastatic CRPC. A major challenge remains the lack of objective criteria to assess response of disease confined to the bone marrow, which is common in individuals with advanced prostate cancer (13,14).

Assessment of Soft-Tissue Disease Response

Prostate Cancer Working Group 3 criteria include the Response Evaluation Criteria in Solid Tumors (RECIST), version 1.1, applied to conventional CT and MRI to assess the treatment response of soft-tissue disease in patients with advanced

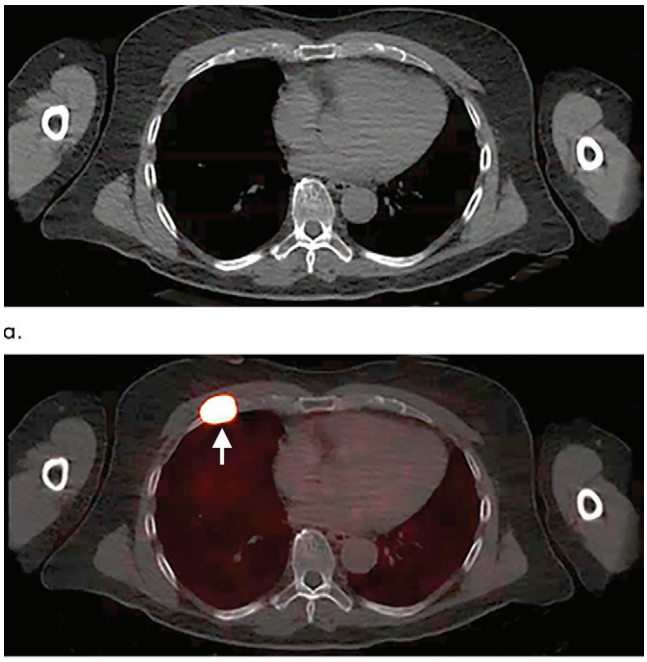

Figure 7: Gallium 68 (^{68}Ga) PET targeting the prostate-specific membrane antigen (PSMA) enables detection of oligorecurrent rib metastasis in a 73-year-old patient with castration-resistant prostate cancer 3 years after initiation of androgen deprivation therapy. **(a, b)** Axial unenhanced CT (**a**) and ^{68}Ga PSMA PET (**b**) images show a solitary site of recurrence (arrow) in the right fourth rib on **b** that is difficult to discern on **a**. Surgical rib resection enabled confirmation of metastatic prostate cancer. The serum prostate-specific antigen level became undetectable after surgery.

prostate cancer. This relies on accurate measurements of summated tumor diameters to categorize therapeutic effects. In the clinical trial setting, whole-body MRI, as well as PET/CT and PET/MRI with a range of radiopharmaceuticals, are investigated for treatment response assessment in patients with soft-tissue and bone disease. These are discussed in the next section.

Assessing Response of Bone Metastases

Radionuclide bone scan.—When evaluating therapeutic benefits in bone metastases, bone scanning is widely used as part of the validated Prostate Cancer Working Group 3 criteria (51) to determine disease progression after treatment. These criteria require identification of at least two new bone lesions in consecutive bone scans performed 9–12 weeks apart; if detected, the new bone lesions need to be confirmed with a subsequent bone scan performed a minimum of 6 weeks later to confirm progression. This is because the osteoblastic flare phenomenon may occur during bone healing (Fig 9) (51). Identification of new lesions is suboptimal in patients with diffuse disease showing generalized increased tracer uptake.

These criteria have substantial limitations given recent imaging advances. *(a)* There is a reliance on bone scanning to depict new metastases, and this modality is less sensitive than PET/CT, PET/MRI, or whole-body MRI. *(b)* Bone scanning is unable to define new bone lesions in patients with diffuse bone involvement. *(c)* Bone scanning must be repeated 6–12 weeks after the first bone scan to confirm disease progression, thereby prolonging patient exposure to the toxicities of nonefficacious treatment. *(d)* Enlargement of bone lesions does not qualify as a progression criterion. *(e)* The Prostate Cancer Working Group 3 criteria document bone disease progression but have no direct measure of treatment benefit. Nevertheless, this method of defining radiographic progression-free survival for bone disease, in combination with modified RECIST, version 1.1, for soft-tissue disease, has been shown to correlate with overall disease survival (64) and is widely adopted in clinical trials.

The bone scan index is a semiquantitative index. It is a method of expressing the tumor burden in bone as a percentage of total skeletal mass. The bone scan index can facilitate comparison of results across measurement time points and institutions. Studies have shown that the bone scan index is prognostic, both at baseline (65) and at follow-up, with patients who have a smaller increase in bone scan index during treatment having longer overall survival (66). However, the bone scan index still does not overcome the issue of flare phenomenon, nor can it enable direct assessment of treatment benefit.

Radiopharmaceuticals for PET imaging.—Interesting results are emerging from small studies in which PET/CT or PET/MRI were used with different radiopharmaceuticals. ^{18}F NaF PET/CT has shown good measurement variability with coefficients of variation for maximum (14.1%) and mean (6.6%) standardized uptake values (SUVs) (67). Harmon et al (68) found that patients who showed disease progression at ^{18}F NaF PET/CT by measuring the functional SUV disease burden have shorter progression-free survival. However, similar to bone scanning, the flare response (ie, increased tracer activity related to treatment) may confound assessments. Likewise, ^{18}F NaF PET/CT appears to be more useful in the detection of disease progression, as there are no universally accepted response criteria, and the technique is not used to assess soft-tissue disease.

PET/CT with choline radiolabeled with either ^{18}F or ^{11}C and PSMA radiolabeled with either ^{68}Ga or ^{18}F has the advantage of enabling one to assess soft-tissue disease and bone disease at the same time. Several studies have also shown that ^{18}F choline PET/CT can depict disease progression earlier than conventional CT and bone scanning. Decreases in SUV correlate with overall survival (69–71). Flare response may also be observed early after the start of therapy (69). A potential limitation of choline PET/CT is the poor visualization of liver metastases due to high normal liver background tracer uptake.

A recent study assessed bone response to chemotherapy with ^{68}Ga PSMA PET/CT (72). Inhibition of the androgen receptor (eg, by androgen deprivation therapy drug treatment) can markedly increase PSMA expression (73). This can limit the usefulness of this technique in monitoring the therapeutic effects of androgen deprivation therapy.

Whole-body MRI (including DW MRI).—DW MRI is a technique that does not require intravenous contrast material injection and provides insight into tumor cellularity and tumor cell kill. By combining anatomic and functional imaging, whole-body DW MRI can be used to assess tumor response without the confounder of flare phenomenon. Whole-body DW MRI can also depict complications, such as malignant spinal cord compression, fractures, or genitourinary tract obstructions. Evidence is accumulating for the value of whole-body DW MRI in the assessment of therapeutic response (74–76). Two quantitative parameters derived from whole-body DW MRI—apparent diffusion coefficient value and tumor diffusion volume—have been shown to correlate with circulating biomarkers and clinical response to olaparib (an inhibitor of the enzyme poly [ADP-ribose] polymerase, also known as a PARP inhibitor) in individuals with advanced prostate cancer (Fig 10) (74). The recently published MET-RADS-P criteria (44) combine RECIST version 1.1 for soft-tissue assessment with new DW MRI bone metastases response criteria. MET-RADS-P reporting criteria also facilitate the categorization of response to treatment, including any discordant or heterogeneous responses. Application of MET-RADS-P criteria could facilitate the conduct of multicenter clinical trials using whole-body MRI to define better response criteria in patients with bone disease.

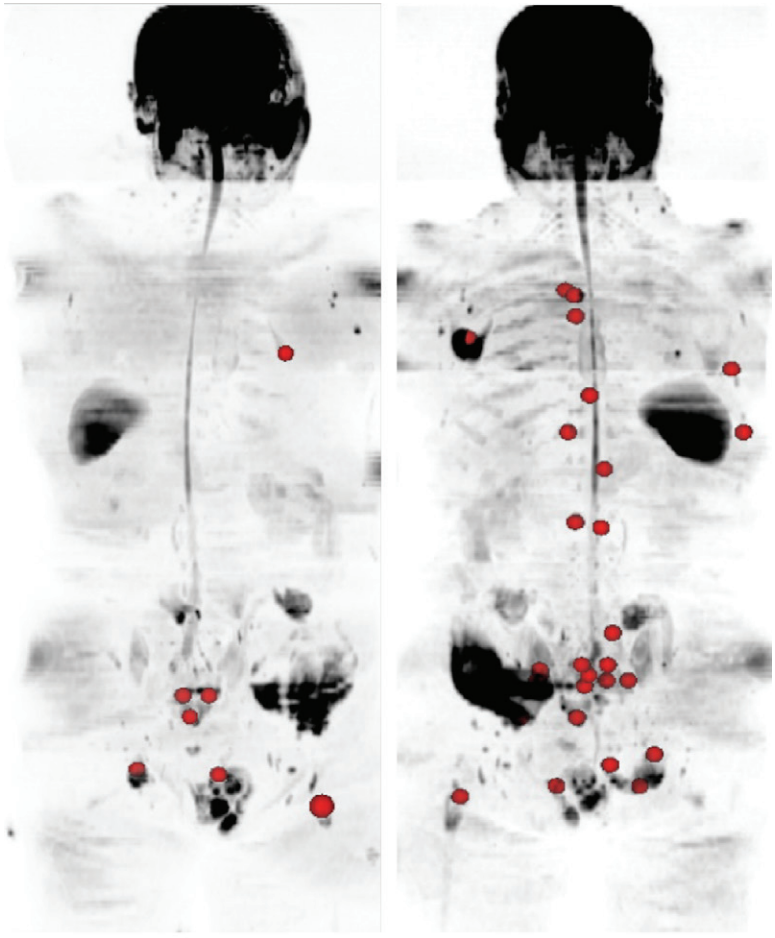

Figure 8: Discordant radiologic and biochemical response in a 68-year-old man with metastatic castration-resistant prostate cancer who had undergone previous treatment with pelvic exenteration for locally advanced prostate cancer and was currently on antiandrogen targeted therapy. Inverted gray-scale coronal maximum intensity projection whole-body diffusion-weighted MRI (*b* value = 900 sec/mm^2) obtained **(a)** before and **(b)** at 12 weeks of treatment shows an increase in the number of bone metastases (color overlay in red), with a contemporaneous reduction in serum prostate-specific antigen (PSA) level from 16 to 4.8 ng/mL. Progression was confirmed 8 weeks later when new bone lesions were seen on a bone scan obtained by using Prostate Cancer Working Group 3 criteria and when new lung metastases were seen on a CT scan (not shown), while the serum PSA level remained low.

Circulating tumor cells.—Concerted efforts are being made to standardize blood circulating tumor cell count as a treatment response criterion. The results from 6081 patients in five prospective randomized phase III trials for blood circulating tumor cell count have been recently reported (77). Changes in circulating tumor cell count measurement before treatment and 13 weeks after treatment were robust and meaningful response end points for early phase metastatic CRPC trials. However, many patients have low circulating tumor cell counts despite having widespread disease. This suggests heterogeneity in the shedding of tumor cells into the blood or the sensitivity of the assay for their detection.

Theranostics: Diagnosing and Treating Advanced Prostate Cancer with Radiopharmaceuticals

Theranostic imaging refers to the combination of an imaging biomarker and a specific targeted therapy with radiopharmaceuticals. The overexpression of PSMA in patients with CRPC has led to the development of PSMA PET/CT tracers as a potential imaging biomarker to guide therapy using PSMA ligand-directed treatments, such as radioimmunoconjugates or immunoconjugates with cytotoxic payloads (78). A number of tracers can be linked for diagnostic (eg, ^{18}F, ^{68}Ga, and ^{89}Zr) or therapeutic (eg, ^{131}I, ^{177}Lu, ^{225}Ac) indications.

The PSMA-targeting theranostic concept offers a new treatment option in patients with CRPC when the ligand is labeled with β-emitting ^{177}Lu or ^{131}I isotopes or an α-emitting ^{225}Ac isotope (79). There is compelling evidence that ^{177}Lu PSMA-617 can lead to a biochemical response (serum PSA reduction of >50%) (80) and improved progression-free survival with relatively low incidence of adverse side-effects in patients with advanced prostate cancer (79,81). A recent meta-analysis of 10 studies comprising 455 patients found that serum PSA decline was observed in 68% of patients after

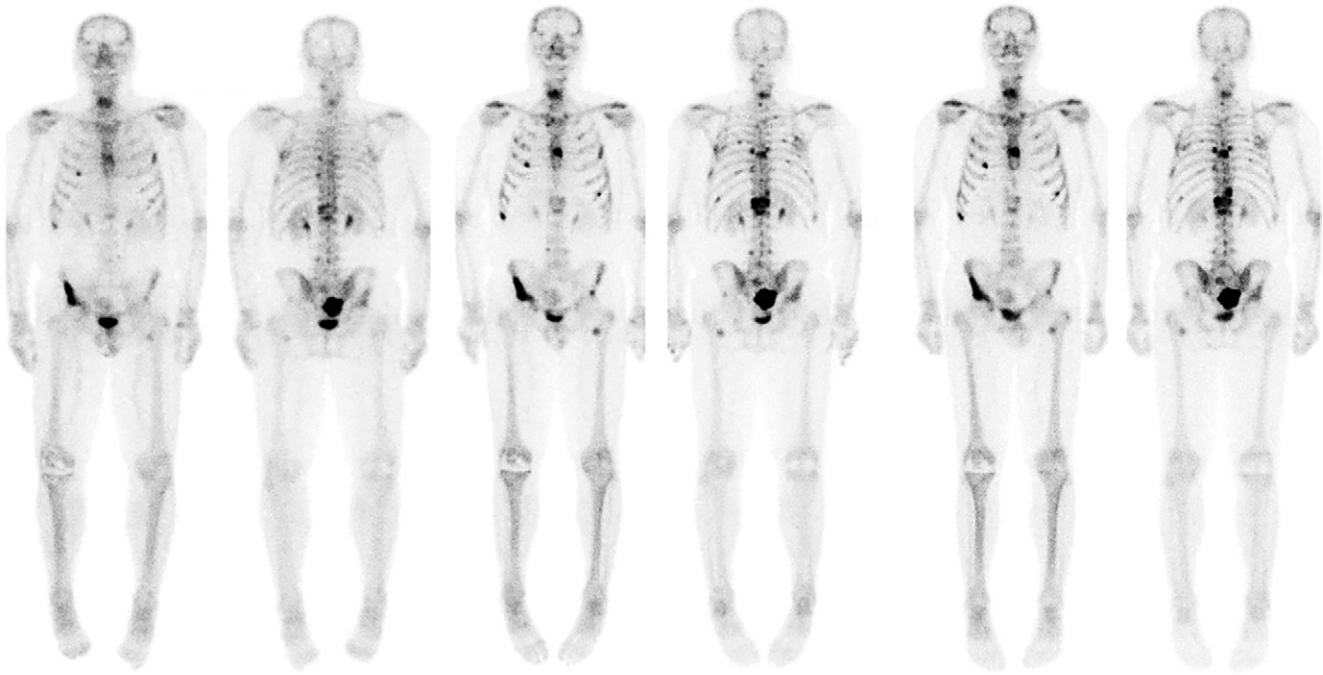

Figure 9: Flare phenomenon was seen on technetium 99m (^{99m}Tc) bone scans 12 weeks after successful therapy in a 64-year-old man with metastatic castration-resistant prostate cancer with bone-only metastases. **(a–c)** Coronal anterior (left) and posterior (right) ^{99m}Tc bone scans obtained at baseline (**a**), 12 weeks (**b**), and 24 weeks (**c**) after therapy. Note the multiple new rib metastases in **b**, with no further new bone lesions in **c**. When the Prostate Cancer Working Group 3 criteria were applied, the criteria for disease progression were not met, and flare phenomenon was documented. A contemporaneous serum prostate-specific antigen response was observed, with 61% reduction at 12 weeks and 69% reduction at 24 weeks.

treatment, with 34% of patients showing a PSA decline of more than 50%. The pooled hazard ratios for the overall survival of any PSA decline was 0.29 ($P < .001$), indicating serum PSA decrease was associated with longer overall survival (82). The incidence of hematologic toxicity (grade III or IV) was reportedly low, comprising anemia (9%), thrombocytopenia (4%), and neutropenia (6%) (83). More recently, it was shown that disease SUV at ^{68}Ga-PSMA PET imaging at baseline screening was predictive of a more than 30% reduction in the serum PSA level (84) after ^{177}Lu PSMA-617 therapy. In addition, a decrease in segmented total tumor volume at ^{68}Ga PSMA PET imaging was associated with serum PSA response after ^{177}Lu PSMA therapy (85). The presence of hepatic disease in patients was associated with poorer serum PSA response, as well as shorter progression-free and overall survival (83). However, the long-term outcomes and efficacy of ^{177}Lu PSMA treatment need to be further validated in prospective clinical trials.

Potential and Challenges of Next-Generation Imaging

There is substantial promise in the use of next-generation imaging to aid the delivery of precision oncology in patients with advanced prostate cancer. Areas in which the greatest potential impact may be seen include *(a)* early and timely detection of biochemical recurrence that may increase the chances of cure, *(b)* more accurate depiction of metastatic tumor burden that has prognostic implications, *(c)* management of oligometastatic disease, and *(d)* earlier detection of response or progression of bone disease to therapy.

In addition, there are opportunities to use novel imaging to advance knowledge of evolving tumor biology. Imaging can be used to study tumor heterogeneity, both within and between tumors. Imaging-targeted tissue sampling will further our understanding of the molecular and genetic profiles associated with treatment resistance, thus guiding therapy selection. The use of PET radiopharmaceuticals, such as PSMA and FDHT, can provide insights into receptor expression and signaling pathways, which may indicate sensitivity or resistance to treatments and can guide the development of future theranostics.

Robust quantitative measurements across imaging platforms are achievable with whole-body DW MRI, as apparent diffusion coefficient measurements have been shown to have good measurement repeatability and reproducibility. However, more studies are needed to validate whole-body MRI measurements as response, predictive, or prognostic biomarkers, including the performance of standardized reporting systems (eg, MET-RADS-P) in the clinical setting. The cost-effectiveness of these modern imaging techniques is also yet to be determined.

Regionally limited availability of novel imaging tracers and the variable imaging expertise across centers constitute major impediments toward the development of validated imaging

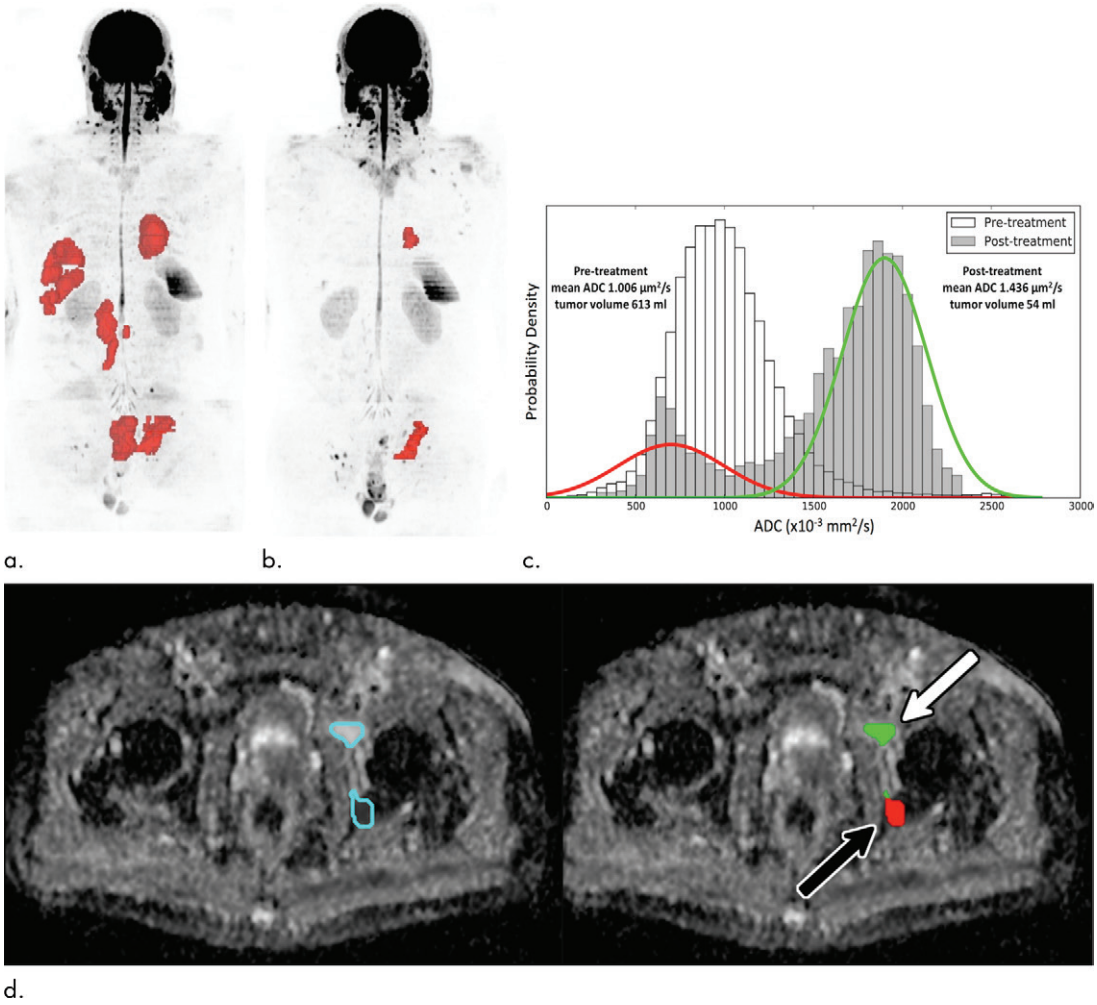

Figure 10: Whole-body MRI shows a response to a targeted therapy (poly [ADP-ribose] polymerase inhibitor). **(a, b)** Images of inverted gray-scale coronal maximum intensity projection (MIP) whole-body diffusion-weighted [DW] MRI (*b* value = 900 sec/mm^2) before (**a**) and 12 weeks after (**b**) treatment in a 70-year-old man with castration-resistant prostate cancer. Color overlay in red shows projection of disease sites before (**a**) and after (**b**) treatment, which are summated to derive the total diffusion volume (tDV, from DW imaging [*b* = 900 sec/mm^2] disease signal) and the associated global apparent diffusion coefficient (ADC) values, as shown in **(c)** the histograms (plotted as probability density on the *y* axis). The images show dramatic reduction in tDV (from 613 mL to 54 mL) accompanied by a marked regression of lung, liver, and nodal metastases, as well as the local prostate tumor. However, there is heterogeneous response, with persistent signal abnormality in the left pelvic bone and the left lung on MIP images. **(d)** Axial posttreatment ADC map through the pelvis shows responding disease (color coded green, ADC > 1.3 μm^2/sec) is visible in the anterior left acetabulum, while nonresponding disease (color coded red, ADC = 0.73 μm^2/sec) is seen in the posterior left acetabulum, accounting for the bimodal distribution of the posttreatment global ADC histogram.

criteria. Furthermore, different classes of drugs used to treat metastatic CRPC may impact imaging in unique ways that are relatively underexplored. Some drug, such as abiraterone or enzalutamide, may change the regulation of the targets for radiopharmaceuticals without killing cancer cells, and such potential effects need to be better understood when selecting modern imaging for treatment response assessment.

In conclusion, next-generation imaging techniques will undoubtedly play increasing roles in defining the presence and extent of metastatic disease and enabling assessment of treatment response and disease progression, particularly in patients with bone disease, and will improve our understanding of disease biology through imaging-targeted tumor sampling. These developments will promote the development and use of precision therapies in patients with advanced prostate cancer, with the aim of improving outcome.

Disclosures of Conflicts of Interest: **R.P.L.** disclosed no relevant relationships. **N.T.** Activities related to the present article: disclosed no relevant relationships. Activities not related to the present article: gave lectures for Janssen, Sanofi, and Bayer. Other relationships: disclosed no relevant relationships. **A.R.P.** disclosed no relevant relationships. **W.J.G.O.** disclosed no relevant relationships. **S.F.** Activities related to the present article: disclosed no relevant relationships. Activities not related to the present article: is a consultant for Bayer; provides expert testimony for Bayer; institution received a grant from Blue Earth; gave lectures for Bayer, Astellas, and BMS; and developed educational presentations for Bayer. Other relationships: disclosed no relevant relationships. **H.A.V.** disclosed no relevant relationships. **A.O.** Activities related to the present article: institution received grants from Teva and Janssen; institution received a consulting fee or honorarium from Astellas, Bayer, Sanofi, Roche, Janssen, MSD, and Molecular Partners; institution received support for travel to meetings for the study or other purposes from Astellas, Bayer, Sanofi, and Janssen. Activities not related to the present article: disclosed no relevant relationships. Other relationships:

disclosed no relevant relationships. **M.J.M.** Activities related to the present article: received a consulting fee from Advanced Accelerator Applications; received support for travel from Endocyte, Bayer, and Progenics. Activities not related to the present article: received research funding from Bayer, Progenics, Corcept, Endocyte, Sanofi, and Janssen. Other relationships: disclosed no relevant relationships. **J.d.B.** disclosed no relevant relationships. **D.M.K.** Activities related to the present article: disclosed no relevant relationships. Activities not related to the present article: is on the Bayer Healthcare Speakers Bureau. Other relationships: disclosed no relevant relationships.

References

1. Cronin KA, Lake AJ, Scott S, et al. Annual report to the nation on the status of cancer, part I: national cancer statistics. Cancer 2018;124(13):2785–2800.
2. Wei L, Wang J, Lampert E, et al. Intratumoral and intertumoral genomic heterogeneity of multifocal localized prostate cancer impacts molecular classifications and genomic prognosticators. Eur Urol 2017;71(2):183–192.
3. Wadosky KM, Koochekpour S. Androgen receptor splice variants and prostate cancer: from bench to bedside. Oncotarget 2017;8(11):18550–18576.
4. Jamaspishvili T, Berman DM, Ross AE, et al. Clinical implications of PTEN loss in prostate cancer. Nat Rev Urol 2018;15(4):222–234.
5. Taylor RA, Fraser M, Livingstone J, et al. Germline BRCA2 mutations drive prostate cancers with distinct evolutionary trajectories. Nat Commun 2017;8:13671.
6. Mateo J, Carreira S, Sandhu S, et al. DNA-repair defects and olaparib in metastatic prostate cancer. N Engl J Med 2015;373(18):1697–1708.
7. Robinson D, Van Allen EM, Wu YM, et al. Integrative clinical genomics of advanced prostate cancer. Cell 2015;162(2):454.
8. National Comprehensive Cancer Network. NCCN Guidelines Version 3.2018: Prostate Cancer. https://www.nccn.org/professionals/physician_gls/pdf/prostate.pdf. Published 2018. Accessed December 1, 2018.
9. Mottet N, Bellmunt J, Bolla M, et al. EAU-ESTRO-SIOG guidelines on prostate cancer. Part 1: screening, diagnosis, and local treatment with curative intent. Eur Urol 2017;71(4):618–629.
10. Tosoian JJ, Gorin MA, Ross AE, Pienta KJ, Tran PT, Schaeffer EM. Oligometastatic prostate cancer: definitions, clinical outcomes, and treatment considerations. Nat Rev Urol 2017;14(1):15–25.
11. De Bleser E, Tran PT, Ost P. Radiotherapy as metastasis-directed therapy for oligometastatic prostate cancer. Curr Opin Urol 2017;27(6):587–595.
12. Mateo J, Fizazi K, Gillessen S, et al. Managing nonmetastatic castration-resistant prostate cancer. Eur Urol 2019;75(2):285–293.
13. James ND, Spears MR, Clarke NW, et al. Survival with newly diagnosed metastatic prostate cancer in the "docetaxel era": data from 917 patients in the control arm of the STAMPEDE trial (MRC PR08, CRUK/06/019). Eur Urol 2015;67(6):1028–1038.
14. Halabi S, Kelly WK, Ma H, et al. Meta-analysis evaluating the impact of site of metastasis on overall survival in men with castration-resistant prostate cancer. J Clin Oncol 2016;34(14):1652–1659.
15. Spratt DE, Zumsteg ZS, Feng FY, Tomlins SA. Translational and clinical implications of the genetic landscape of prostate cancer. Nat Rev Clin Oncol 2016;13(10):597–610.
16. Hövels AM, Heesakkers RA, Adang EM, et al. The diagnostic accuracy of CT and MRI in the staging of pelvic lymph nodes in patients with prostate cancer: a meta-analysis. Clin Radiol 2008;63(4):387–395.
17. Harisinghani MG, Barentsz J, Hahn PF, et al. Noninvasive detection of clinically occult lymph-node metastases in prostate cancer. N Engl J Med 2003;348(25):2491–2499.
18. Briganti A, Larcher A, Abdollah F, et al. Updated nomogram predicting lymph node invasion in patients with prostate cancer undergoing extended pelvic lymph node dissection: the essential importance of percentage of positive cores. Eur Urol 2012;61(3):480–487.
19. Gandaglia G, Fossati N, Zaffuto E, et al. Development and internal validation of a novel model to identify the candidates for extended pelvic lymph node dissection in prostate cancer. Eur Urol 2017;72(4):632–640.
20. Thoeny HC, Barbieri S, Froehlich JM, Turkbey B, Choyke PL. Functional and targeted lymph node imaging in prostate cancer: current status and future challenges. Radiology 2017;285(3):728–743.
21. Thoeny HC, Froehlich JM, Triantafyllou M, et al. Metastases in normal-sized pelvic lymph nodes: detection with diffusion-weighted MR imaging. Radiology 2014;273(1):125–135.
22. Birkhäuser FD, Studer UE, Froehlich JM, et al. Combined ultrasmall superparamagnetic particles of iron oxide-enhanced and diffusion-weighted magnetic resonance imaging facilitates detection of metastases in normal-sized pelvic lymph nodes of patients with bladder and prostate cancer. Eur Urol 2013;64(6):953–960.
23. Thoeny HC, Triantafyllou M, Birkhaeuser FD, et al. Combined ultrasmall superparamagnetic particles of iron oxide-enhanced and diffusion-weighted magnetic resonance imaging reliably detect pelvic lymph node metastases in normal-sized nodes of bladder and prostate cancer patients. Eur Urol 2009;55(4):761–769.
24. Woo S, Suh CH, Kim SY, Cho JY, Kim SH. The diagnostic performance of MRI for detection of lymph node metastasis in bladder and prostate cancer: an updated systematic review and diagnostic meta-analysis. AJR Am J Roentgenol 2018;210(3):W95–W109.
25. Salminen E, Hogg A, Binns D, Frydenberg M, Hicks R. Investigations with FDG-PET scanning in prostate cancer show limited value for clinical practice. Acta Oncol 2002;41(5):425–429.
26. von Eyben FE, Kairemo K. Meta-analysis of (11)C-choline and (18)F-choline PET/CT for management of patients with prostate cancer. Nucl Med Commun 2014;35(3):221–230.
27. Evangelista L, Guttilla A, Zattoni F, Muzzio PC, Zattoni F. Utility of choline positron emission tomography/computed tomography for lymph node involvement identification in intermediate- to high-risk prostate cancer: a systematic literature review and meta-analysis. Eur Urol 2013;63(6):1040–1048.
28. Silver DA, Pellicer I, Fair WR, Heston WD, Cordon-Cardo C. Prostate-specific membrane antigen expression in normal and malignant human tissues. Clin Cancer Res 1997;3(1):81–85.
29. Bravaccini S, Puccetti M, Bocchini M, et al. PSMA expression: a potential ally for the pathologist in prostate cancer diagnosis. Sci Rep 2018;8(1):4254.
30. Bakht MK, Oh SW, Youn H, Cheon GJ, Kwak C, Kang KW. Influence of androgen deprivation therapy on the uptake of PSMA-targeted agents: emerging opportunities and challenges. Nucl Med Mol Imaging 2017;51(3):202–211.
31. Perera M, Papa N, Christidis D, et al. Sensitivity, specificity, and predictors of positive ^{68}Ga-prostate-specific membrane antigen positron emission tomography in advanced prostate cancer: a systematic review and meta-analysis. Eur Urol 2016;70(6):926–937.
32. Maurer T, Gschwend JE, Rauscher I, et al. Diagnostic efficacy of (68)gallium-PSMA positron emission tomography compared to conventional imaging for lymph node staging of 130 consecutive patients with intermediate to high risk prostate cancer. J Urol 2016;195(5):1436–1443.
33. Giesel FL, Knorr K, Spohn F, et al. Detection efficacy of [^{18}F]PSMA-1007 PET/CT in 251 Patients with biochemical recurrence after radical prostatectomy. J Nucl Med 2018 Jul 24 [Epub ahead of print] https://doi.org/10.2967/jnumed.118.212233.
34. Giesel FL, Will L, Kesch C, et al. Biochemical recurrence of prostate cancer: initial results with [^{18}F]PSMA-1007 PET/CT. J Nucl Med 2018;59(4):632–635.
35. Shen G, Deng H, Hu S, Jia Z. Comparison of choline-PET/CT, MRI, SPECT, and bone scintigraphy in the diagnosis of bone metastases in patients with prostate cancer: a meta-analysis. Skeletal Radiol 2014;43(11):1503–1513.
36. Yang HL, Liu T, Wang XM, Xu Y, Deng SM. Diagnosis of bone metastases: a meta-analysis comparing ^{18}FDG PET, CT, MRI and bone scintigraphy. Eur Radiol 2011;21(12):2604–2617.
37. Lecouvet FE, Geukens D, Stainier A, et al. Magnetic resonance imaging of the axial skeleton for detecting bone metastases in patients with high-risk prostate cancer: diagnostic and cost-effectiveness and comparison with current detection strategies. J Clin Oncol 2007;25(22):3281–3287.
38. Parker CC, James ND, Brawley CD, et al. Radiotherapy to the primary tumour for newly diagnosed, metastatic prostate cancer (STAMPEDE): a randomised controlled phase 3 trial. Lancet 2018;392(10162):2353–2366.
39. Jambor I, Kuisma A, Ramadan S, et al. Prospective evaluation of planar bone scintigraphy, SPECT, SPECT/CT, 18F-NaF PET/CT and whole body 1.5T MRI, including DWI, for the detection of bone metastases in high risk breast and prostate cancer patients: SKELETA clinical trial. Acta Oncol 2016;55(1):59–67.
40. Lecouvet FE, El Mouedden J, Collette L, et al. Can whole-body magnetic resonance imaging with diffusion-weighted imaging replace Tc 99m bone scanning and computed tomography for single-step detection of metastases in patients with high-risk prostate cancer? Eur Urol 2012;62(1):68–75.
41. Gutzeit A, Doert A, Froehlich JM, et al. Comparison of diffusion-weighted whole body MRI and skeletal scintigraphy for the detection of bone metastases in patients with prostate or breast carcinoma. Skeletal Radiol 2010;39(4):333–343.
42. Pasoglou V, Larbi A, Collette L, et al. One-step TNM staging of high-risk prostate cancer using magnetic resonance imaging (MRI): toward an upfront simplified "all-in-one" imaging approach? Prostate 2014;74(5):469–477.
43. Dyrberg E, Hendel HW, Huynh THV, et al. ^{68}Ga-PSMA-PET/CT in comparison with ^{18}F-fluoride-PET/CT and whole-body MRI for the detection of bone metastases in patients with prostate cancer: a prospective diagnostic accuracy study. Eur Radiol 2019;29(3):1221–1230.
44. Padhani AR, Lecouvet FE, Tunariu N, et al. METastasis Reporting and Data System for Prostate Cancer: practical guidelines for acquisition, interpretation, and reporting of whole-body magnetic resonance imaging-based

evaluations of multiorgan involvement in advanced prostate cancer. Eur Urol 2017;71(1):81–92.
45. Barnes A, Alonzi R, Blackledge M, et al. UK quantitative WB-DWI technical workgroup: consensus meeting recommendations on optimisation, quality control, processing and analysis of quantitative whole-body diffusion-weighted imaging for cancer. Br J Radiol 2018;91(1081):20170577.
46. Robertson NL, Sala E, Benz M, et al. Combined whole body and multiparametric prostate magnetic resonance imaging as a 1-step approach to the simultaneous assessment of local recurrence and metastatic disease after radical prostatectomy. J Urol 2017;198(1):65–70.
47. Tateishi U, Morita S, Taguri M, et al. A meta-analysis of (18)F-fluoride positron emission tomography for assessment of metastatic bone tumor. Ann Nucl Med 2010;24(7):523–531.
48. Wondergem M, van der Zant FM, van der Ploeg T, Knol RJ. A literature review of 18F-fluoride PET/CT and 18F-choline or 11C-choline PET/CT for detection of bone metastases in patients with prostate cancer. Nucl Med Commun 2013;34(10):935–945.
49. Pyka T, Okamoto S, Dahlbender M, et al. Comparison of bone scintigraphy and ^{68}Ga-PSMA PET for skeletal staging in prostate cancer. Eur J Nucl Med Mol Imaging 2016;43(12):2114–2121.
50. Larson SM, Morris M, Gunther I, et al. Tumor localization of 16beta-18F-fluoro-5alpha-dihydrotestosterone versus 18F-FDG in patients with progressive, metastatic prostate cancer. J Nucl Med 2004;45(3):366–373.
51. Scher HI, Morris MJ, Stadler WM, et al. Trial design and objectives for castration-resistant prostate cancer: updated recommendations from the prostate cancer clinical trials working group 3. J Clin Oncol 2016;34(12):1402–1418.
52. Ren J, Yuan L, Wen G, Yang J. The value of anti-1-amino-3-18F-fluorocyclobutane-1-carboxylic acid PET/CT in the diagnosis of recurrent prostate carcinoma: a meta-analysis. Acta Radiol 2016;57(4):487–493.
53. Bach-Gansmo T, Nanni C, Nieh PT, et al. Multisite experience of the safety, detection rate and diagnostic performance of fluciclovine (^{18}F) positron emission tomography/computerized tomography imaging in the staging of biochemically recurrent prostate cancer. J Urol 2017;197(3 Pt 1):676–683.
54. Joice GA, Rowe SP, Pienta KJ, Gorin MA. Oligometastatic prostate cancer: shaping the definition with molecular imaging and an improved understanding of tumor biology. Curr Opin Urol 2017;27(6):533–541.
55. Larbi A, Dallaudière B, Pasoglou V, et al. Whole body MRI (WB-MRI) assessment of metastatic spread in prostate cancer: therapeutic perspectives on targeted management of oligometastatic disease. Prostate 2016;76(11):1024–1033.
56. Ost P, Jereczek-Fossa BA, As NV, et al. Progression-free survival following stereotactic body radiotherapy for oligometastatic prostate cancer treatment-naive recurrence: a multi-institutional analysis. Eur Urol 2016;69(1):9–12.
57. Murphy DG, Sweeney CJ, Tombal B. "Gotta catch 'em all", or do we? Pokemet approach to metastatic prostate cancer. Eur Urol 2017;72(1):1–3.
58. Palma DA, Salama JK, Lo SS, et al. The oligometastatic state: separating truth from wishful thinking. Nat Rev Clin Oncol 2014;11(9):549–557.
59. Eyben FE, Picchio M, von Eyben R, Rhee H, Bauman G. ^{68}Ga-labeled prostate-specific membrane antigen ligand positron emission tomography/computed tomography for prostate cancer: a systematic review and meta-analysis. Eur Urol Focus 2018;4(5):686–693.
60. Mapelli P, Incerti E, Ceci F, Castellucci P, Fanti S, Picchio M. 11C- or 18F-choline PET/CT for imaging evaluation of biochemical recurrence of prostate cancer. J Nucl Med 2016;57(Suppl 3):43S–48S.
61. Evangelista L, Zattoni F, Karnes RJ, Novara G, Lowe V. Radiolabeled choline PET/CT before salvage lymphadenectomy dissection: a systematic review and meta-analysis. Nucl Med Commun 2016;37(12):1223–1231.
62. Gillessen S, Attard G, Beer TM, et al. Management of patients with advanced prostate cancer: the report of the advanced prostate cancer consensus conference APCCC 2017. Eur Urol 2018;73(2):178–211.
63. Bryce AH, Alumkal JJ, Armstrong A, et al. Radiographic progression with nonrising PSA in metastatic castration-resistant prostate cancer: post hoc analysis of PREVAIL. Prostate Cancer Prostatic Dis 2017;20(2):221–227.
64. Morris MJ, Molina A, Small EJ, et al. Radiographic progression-free survival as a response biomarker in metastatic castration-resistant prostate cancer: COU-AA-302 results. J Clin Oncol 2015;33(12):1356–1363.
65. Nakajima K, Edenbrandt L, Mizokami A. Bone scan index: a new biomarker of bone metastasis in patients with prostate cancer. Int J Urol 2017;24(9):668–673.
66. Reza M, Ohlsson M, Kaboteh R, et al. Bone scan index as an imaging biomarker in metastatic castration-resistant prostate cancer: a multicentre study based on patients treated with abiraterone acetate (zytiga) in clinical practice. Eur Urol Focus 2016;2(5):540–546.
67. Lin C, Bradshaw T, Perk T, et al. Repeatability of quantitative 18F-NaF PET: a multicenter study. J Nucl Med 2016;57(12):1872–1879.
68. Harmon SA, Perk T, Lin C, et al. Quantitative assessment of early [^{18}F] sodium fluoride positron emission tomography/computed romography response to treatment in men with metastatic prostate cancer to bone. J Clin Oncol 2017;35(24):2829–2837.
69. De Giorgi U, Caroli P, Burgio SL, et al. Early outcome prediction on 18F-fluorocholine PET/CT in metastatic castration-resistant prostate cancer patients treated with abiraterone. Oncotarget 2014;5(23):12448–12458.
70. De Giorgi U, Caroli P, Scarpi E, et al. (18)F-fluorocholine PET/CT for early response assessment in patients with metastatic castration-resistant prostate cancer treated with enzalutamide. Eur J Nucl Med Mol Imaging 2015;42(8):1276–1283 [Published correction appears in Eur J Nucl Med Mol Imaging 2015;42(8):1337–1338.] https://doi.org/10.1007/s00259-015-3042-5.
71. Ceci F, Herrmann K, Hadaschik B, Castellucci P, Fanti S. Therapy assessment in prostate cancer using choline and PSMA PET/CT. Eur J Nucl Med Mol Imaging 2017;44(Suppl 1):78–83.
72. Seitz AK, Rauscher I, Haller B, et al. Preliminary results on response assessment using ^{68}Ga-HBED-CC-PSMA PET/CT in patients with metastatic prostate cancer undergoing docetaxel chemotherapy. Eur J Nucl Med Mol Imaging 2018;45(4):602–612.
73. Hope TA, Truillet C, Ehman EC, et al. 68Ga-PSMA-11 PET imaging of response to androgen receptor inhibition: first human experience. J Nucl Med 2017;58(1):81–84.
74. Perez-Lopez R, Mateo J, Mossop H, et al. Diffusion-weighted imaging as a treatment response biomarker for evaluating bone metastases in prostate cancer: a pilot study. Radiology 2017;283(1):168–177.
75. Blackledge MD, Tunariu N, Orton MR, et al. Inter- and intra-observer repeatability of quantitative whole-body, diffusion-weighted imaging (WB-DWI) in metastatic bone disease. PLoS One 2016;11(4):e0153840.
76. Blackledge MD, Collins DJ, Tunariu N, et al. Assessment of treatment response by total tumor volume and global apparent diffusion coefficient using diffusion-weighted MRI in patients with metastatic bone disease: a feasibility study. PLoS One 2014;9(4):e91779.
77. Heller G, McCormack R, Kheoh T, et al. Circulating tumor cell number as a response measure of prolonged survival for metastatic castration-resistant prostate cancer: a comparison with prostate-specific antigen across five randomized phase III clinical trials. J Clin Oncol 2018;36(6):572–580.
78. Hofman MS, Murphy DG, Williams SG, et al. A prospective randomized multicentre study of the impact of gallium-68 prostate-specific membrane antigen (PSMA) PET/CT imaging for staging high-risk prostate cancer prior to curative-intent surgery or radiotherapy (proPSMA study): clinical trial protocol. BJU Int 2018;122(5):783–793.
79. Virgolini I, Decristoforo C, Haug A, Fanti S, Uprimny C. Current status of theranostics in prostate cancer. Eur J Nucl Med Mol Imaging 2018;45(3):471–495.
80. Ferdinandus J, Eppard E, Gaertner FC, et al. Predictors of response to radioligand therapy of metastatic castrate-resistant prostate cancer with 177Lu-PSMA-617. J Nucl Med 2017;58(2):312–319.
81. Hofman MS, Violet J, Hicks RJ, et al. [^{177}Lu]-PSMA-617 radionuclide treatment in patients with metastatic castration-resistant prostate cancer (LuPSMA trial): a single-centre, single-arm, phase 2 study. Lancet Oncol 2018;19(6):825–833.
82. Kim YJ, Kim YI. Therapeutic responses and survival effects of 177Lu-PSMA-617 radioligand therapy in metastatic castrate-resistant prostate cancer: a meta-analysis. Clin Nucl Med 2018;43(10):728–734.
83. Heck MM, Tauber R, Schwaiger S, et al. Treatment outcome, toxicity, and predictive factors for radioligand therapy with ^{177}Lu-PSMA-I&T in metastatic castration-resistant prostate cancer. Eur Urol 2018 Nov 22 [Epub ahead of print].
84. Emmett L, Crumbaker M, Ho B, et al. Results of a prospective phase 2 pilot trial of ^{177}Lu-PSMA-617 therapy for metastatic castration-resistant prostate cancer including imaging predictors of treatment response and patterns of progression. Clin Genitourin Cancer 2019;17(1):15–22.
85. Grubmüller B, Senn D, Kramer G, et al. Response assessment using ^{68}Ga-PSMA ligand PET in patients undergoing ^{177}Lu-PSMA radioligand therapy for metastatic castration-resistant prostate cancer. Eur J Nucl Med Mol Imaging 2018 Dec 19 [Epub ahead of print] https://doi.org/10.1007/s00259-018-4236-4.